European Journal of Soil Science, June 2007, **58,** 609–624 doi: 10.1111/j.1365-2389.2006.00846.x

Application of two surface complexation models to the adsorption of weak organic acids by soil: an additive approach

R. CALVET[a], E. BARRIUSO[a] & I. G. DUBUS[b]
[a]*Institut National de la Recherche Agronomique (Unité Environnement et Grandes Cultures), 78850 Thiverval-Grignon, and*
[b]*Bureau de Recherche Géologique et Minière, Water Division, 45060 Orléans, France*

Summary

The description of adsorption of organic acids by soil with models requires many parameters. It is often difficult to obtain their values, and so we might try to test the application of models with published data on soil characteristics. We used two models in our trials, namely the constant capacitance model and the variable surface charge–variable surface potential model. We modelled the sorption data for three weak organic acids [2,4-D, 2–4-dichloro-phenoxy acetic acid; salicylic acid, 2-hydroxybenzoic acid; and clofencet, 2–4-(chlorophenyl)-3-ethyl-2,5-dihydro-5-oxopyridazine-4-carboxylic acid] in three Cambisols and two Ferralsols. We adopt an additive approach where the five soils were considered to behave as mixtures of goethite and gibbsite. This was done with values taken from the literature on the assumption that the compounds formed monodentate complexes. Variations given by the two models in adsorbed amounts as a result of pH changes were well described for clofencet and 2,4-D but were less successful for salicylic acid. Simulations of sorption isotherms at various pHs ranging from 5 to 8 matched the experimental data closely for clofencet. Prediction of the adsorption of clofencet and 2,4-D in a range of Cambisols and Ferralsols at their native pH was generally good. We attribute the somewhat poorer fit observed for salicylic acid to the formation of bidendate complexes. Further improvement to the modelling should involve the formation of bidentate complexes between organic acids and oxide material and the effects of organic matter, particularly in relation to adsorption of non-ionized compounds.

Introduction

Adsorption of organic acids involves both ionized and non-ionized forms of the compounds and depends therefore on several physicochemical factors that influence the ionization of those acids and that of surface functional groups, such as pH. The influence of pH on anion adsorption is typically described on the basis of surface complexation and electrostatic interactions with positive electric charges on mineral surfaces such as those of aluminium and iron oxides and hydroxides (e.g. Parfitt *et al*., 1977a,b; Hingston, 1981). In contrast, the adsorption of non-ionized forms of ionizable compounds is associated mainly with organic matter through polar and hydrophobic interactions, but may also be due to complexation on sesquioxide surfaces (Horanyi, 2002). The modelling of anion adsorption has been widely developed, especially for inorganic anions such as nitrate, arsenate, arsenite and phosphate. Several models giving more or less detailed descriptions of the mineral solution interface have been proposed (Goldberg, 1992). Comparative studies suggest that no model is generally better than the others with regard to the description of the charging process of the mineral surface and the adsorption of inorganic anions (Westall & Hohl, 1980; Barrow & Bowden, 1987). Some questions remain about their physicochemical meaning and their ability to describe correctly the mechanisms at a molecular level. The distinction between inner and outer sphere complexes could be questioned (Goldberg, 2005), and according to several authors they are essentially data fitting models (Lützenkirchen, 1999; Zuyi *et al*., 2000). In spite of these questions, models have been widely used and have described successfully numerous experimental results (Goldberg, 1992).

Surface complexation models have been applied principally to the adsorption of single anions on oxide and hydroxide surfaces. Describing ion adsorption on whole soils or sediments remains a challenge. Difficulties encountered include: (i) the competition

Correspondence: E. Barriuso. E-mail: barriuso@grignon.inra.fr
Received 19 January 2006; revised version accepted 16 May 2006

for adsorption sites (Gustafsson, 2001); (ii) the presence of different heterogeneous surfaces; and (iii) the heterogeneity of materials due to the variety of organic and mineral constituents and to their own surface heterogeneity. With regard to the last aspect, several approaches have been adopted to deal with heterogeneity (Barrow *et al*., 1993; Barrow, 1999). Heterogeneity may be taken into account at the level of the constituents themselves or as the assemblages of them. Examples of the former approach are descriptions that consider several adsorbing sites (Tadanier & Eick, 2002). Examples of approaches where the heterogeneity is considered at the assemblage level include: (i) the additive approach (Davis *et al*., 1998), where the total adsorption is assumed to be represented by the sum of the adsorption on individual soil constituents, which are assumed to behave independently; and (ii) global description approaches that consider distribution functions of soil properties or mean values characterizing key soil properties. Examples of the latter include the assignment of normal distributions to surface electric potentials for phosphate adsorption (Barrow, 1983) and the use of relationships between the surface equilibrium complexation constants of boron and several soil properties (Goldberg *et al*., 2000).

We wanted to evaluate the potential for application of surface complexation models to soils using the additivity approach. The two models considered were the constant capacitance model (CC model) and the Stern model of variable surface charge–variable surface potential (VSC VSP model). In contrast to traditional approaches in which models are calibrated against experimental data to obtain a good fit to the observations, we wanted to evaluate the predictive potential for modelling the adsorption of weak organic acids on several contrasting soils using parameter values taken from the literature (i.e. without resorting to a calibration step). We assumed that the adsorption of organic acids in soils could be attributed mostly to oxide and hydroxide minerals, and so we took the additive approach. This hypothesis was also used to model the adsorption of organic chemicals on soil (Davis *et al*., 1998), to describe competitive anion adsorption on oxide minerals and allophanes (Gustafsson, 2001) and to simulate the surface electric charge density of a soil (Taubaso *et al*., 2004). We used experimental data on the adsorption of the three organic acids (2,4-D, clofencet and salicylic acid) on five soils (Dubus *et al*., 2001).

Materials and methods

Five soils as described briefly below were used. The 'Fertans' soil is a humic Cambisol sampled in a plot under permanent grass in the Jura region of France; the 'Maves' (Loir et Cher, France) and 'Villeroy' (Yonne, France) samples (calcic Cambisols) are typical of the main areas of cereal cultivation in France. The two Ferralsols were sampled in New Caledonia, South Pacific, and have been classified as Ferralitic ferritic (Ouénarou) and Ferralitic allitic (Maré) (Table 1). Aluminium and iron speciation were characterized by the Tamm and Mehra–Jackson extraction methods (Mehra & Jackson, 1960; Jeanroy, 1983). The oxalate reagent of the Tamm method extracts Al-organic complexes, Al amorphous hydroxides, allophanes, and amorphous and poorly crystallized Fe hydroxides, while the dithionite–citrate–bicarbonate (dcb) reagent method of Mehra and Jackson allows the extraction of well-crystallized Fe oxides together with amorphous and poorly crystallized Fe hydroxides and allophanes (Jeanroy, 1983). Well-crystallized Al hydroxides are not extracted with the dcb method and only partly extracted by the oxalate reagent (Parfitt & Childs, 1988).

Results on Fe and Al extraction were used to estimate the amount of different oxides (Table 2). Cambisols (Fertans, Maves and Villeroy) were found to contain small amounts of sesquioxides. Goethite can be expected to be the main Fe oxide in Cambisols (Duchaufour, 1995). Clay contents of these soils

Table 1 Physico-chemical properties of soils considered

Sampling location	Soil type	Clay	Silt	Organic C	pH	CEC pH 7	Oxalate extractable		Dithionite-citrate-bicarbonate extractable	
			g/kg^{-1}		(H_2O)	$/mmol_c\ kg^{-1}$	m_{Al}	m_{Fe}	m_{Al} $/g\ kg^{-1}$	m_{Fe}
Fertans, Jura, France	Humic Cambisol	571	367	50.4	6.3	511	4.1	6.0	6.9	39.8
Maves, Yonne, France	Calcic Cambisol	357	565	13.9	6.6	211	1.2	1.8	1.8	11.7
Villeroy, Loir et Cher, France	Calcic Cambisol	237	622	16.7	7.0	131	0.7	2.4	1.1	9.1
Ouénarou, Grande Terre, New Caledonia	Ferralitic ferritic Ferralsol	283	280	36.5	5.2	66	1.0	2.2	20.9	217.4
Maré island, New Caledonia	Ferralitic allitic Ferralsol	259	524	93.4	7.2	488	14.2	4.8	33.8	97.8

Table 2 Contents of oxide for the five soils; m_{go}, m_{gi} and m_{ox} are the contents of goethite, gibbsite and total oxides, respectively. All contents are expressed in kg kg^{-1}

Soil	m_{go}	m_{gi}	m_{ox}
Fertans	0.0633	0.0118	0.0752
Maves	0.0186	0.0035	0.0221
Villeroy	0.0145	0.0020	0.0165
Ouénarou	0.3459	0.0029	0.3488
Maré	0.1556	0.7470	0.9026

ranged from 237 to 571 g kg^{-1}, where 2:1 minerals are dominant (Duchaufour, 1995). As expected, oxide contents were much larger in Ferralsols (Ouénarou and Maré) than in Cambisols. Ferralitic-ferritic soils from New Caledonia are formed on peridotite rocks (Schwertmann & Latham, 1986; Becquer *et al*., 2001). They are rich in goethite, contain small amounts of other metallic (Mn, Cr, V, Ni) oxides and contain very little silica, alumina and neoformed clays. In these soils, the amount of Fe extracted by the dcb reagent usually represents 90–100% of the total Fe of the soil and corresponds to approximately equivalent amounts of goethite and haematite (Becquer *et al*., 2001). Al-crystallized hydroxides were not identified in these soils, which suggests that Al extracted from the Ouénarou sample with oxalate probably originates from amorphous hydroxides, which represent less than 5% of the total oxi-hydroxide amount of the soils. The Ferralitic-allitic soil sampled on the Maré island is derived from the weathering of volcanic ashes deposited on coral rock (Becquer *et al*., 2001). Iron is present in this soil as goethite, while aluminium is present largely as gibbsite with some boehmite. An estimation of the amount of Al- hydroxides in the soil was obtained from the amount of Al extracted with the oxalate reagent (m_{Alo}) and the ratio of $m_{Alo}/m_{Al_2O_3}$ (0.019 ± 0.03) observed for soils from the same location (Becquer *et al*., 2001). This led to an estimated Al-hydroxide content of 0.747 kg kg^{-1}.

For applying the two models, we assumed that the various soils could be represented by 'equivalent soils' made of mixtures of goethite and gibbsite (additivity approach). We made the following underlying assumptions.

1 Naturally occurring goethite and haematite and their synthetic equivalents have similar physico-chemical properties with regard to anion adsorption.

2 Amorphous sesquioxides behave like crystallized oxides with regard to anion adsorption.

3 The properties for gibbsite can be used for describing those of natural Al hydroxides.

4 Oxihydroxides of Cambisols and Ferralsols have similar properties and the two groups of soils only differ by their amounts of Al and Fe minerals.

5 The impact of clays on anion adsorption may be neglected considering their low anion adsorption capacity and because they are generally coated by oxides, hydroxides or organic matter.

Three weak organic acids were used: clofencet (2–4-(chlorophenyl)-3-ethyl-2,5-dihydro-5-oxopyridazine-4-carboxylic acid), a wheat hybridizing agent, 2,4-D (2–4-dichloro-phenoxy acetic acid) and salicylic acid (2-hydroxybenzoic acid). Salicylic acid and 2,4-D were uniformly labelled with ^{14}C on their phenyl ring (specific activity 370×10^9 Bq mol^{-1} and 740×10^9 Bq mol^{-1}, respectively) and were purchased from Sigma France. The labelled ^{14}C was on the pyridazine ring for clofencet (specific activity 1.2×10^{12} Bq mol^{-1}) and was supplied by Monsanto. Carboxylic functions have similar dissociation constants for the three compounds (pK_a 2.6–2.8). Salicylic acid has a second pK_a at 13.4 corresponding to the phenolic OH dissociation.

For adsorption experiments, 5 g of air-dried soil sieved to pass 2 mm were suspended in 10 ml of a solution of ^{14}C-labelled chemical in a 0.01 M $CaCl_2$ background electrolyte. From preliminary measurements we assumed that equilibrium was reached within 24 hours, during which the mixture was shaken in the dark at 25 ± 1°C. The liquid phase was then recovered by centrifugation at 5000 ***g***. We investigated the influence of pH on adsorbed amounts by varying the pH in the suspension by addition of either 0.1 M NaOH or 0.1 M HCl solutions. Suspensions were allowed to equilibrate for 4 hours before addition of solutions of the three organic acids. The resulting initial organic acid concentration was 10 mg $litre^{-1}$. In addition, adsorption isotherms of clofencet on the Maves and Villeroy soils were established at several pHs between 5.0 and 8.5, with initial concentrations ranging from 1 to 30 mg $litre^{-1}$.

Theory and application of the constant capacitance model (CC model)

Model theory

The constant capacitance model of the interface between the oxide mineral and aqueous solution was developed by Schindler and Stumm (Goldberg, 1992) and is based on the following hypotheses.

1 All surface complexes are inner-sphere complexes with anion adsorption resulting from ligand exchange reactions.

2 The constant ionic medium determines the activity coefficients of the aqueous species that appear in the expression of the equilibrium constant.

3 No complexes are formed with the ions of the background electrolyte.

4 A linear relationship exists between the surface electric charge and the surface electric potential.

The ionization of surface OH groups and surface complexation reactions of a ligand L are described by the following equations:

$$SOH + H^+ \rightleftarrows SOH_2^+ \quad (1)$$

$$SOH \rightleftarrows SO^- + H^+ \quad (2)$$

$$SOH + L^{n-} \rightleftarrows SL^{(n-1)-} + OH^- \quad (3)$$

and

$$2SOH + L^{n-} \rightleftarrows S_2L^{(n-2)-} + 2OH^- \quad (4)$$

where SOH is a surface OH group, L is a ligand and n is the charge on the ligand.

The nature of surface complexes, either monodentate or bidentate, is not yet definitely established and appears to depend on the nature of the organic acids as shown by several published results. The adsorption of aliphatic carboxylic acids on Fe hydroxide has been interpreted in terms of the two types of complexes, monodentate and bidentate (Cornell & Schindler, 1980). Other investigators studying the adsorption of phosphate, oxalate and benzoate have concluded that there is a formation of surface monodentate complexes on goethite and possibly monodentate and bidentate complexes on gibbsite (Parfitt *et al*., 1977a, 1977b). The nature of the complex formed for salicylic acid depends on pH conditions, monodendate complexes being prevalent under neutral conditions and bidendate complexes more common in acid media, as shown by ATR-FTIR spectroscopy (Kubicki *et al*., 1997). Nevertheless, the adsorption of these organic acids can be adequately simulated on the basis of the formation of monodentate surface complexes only (Goldberg, 1992). Surface reactions are frequently expressed in terms of undissociated acids.

For an acid HL:

$$SOH + HL \rightleftarrows SL + H_2O. \quad (5)$$

For an acid H_2L:

$$SOH + H_2L \rightleftarrows SHL + H_2O, \quad (6)$$

and

$$SOH + H_2L \rightleftarrows SL^- + H_2O + H^+. \quad (7)$$

The description of adsorption by the constant capacitance model involves several equations that are described in Appendix 1.

Derivation of the intrinsic equilibrium constant K_L^1*(int)*

The CC model was applied to adsorption of the three organic acids on soils with the following assumptions.

1 The three compounds behave as monoprotic acids, which is true for 2,4-D and clofencet, and which is considered an acceptable approximation for salicylic acid because of its large second pK_a value (13.4).

2 Adsorption is due to the formation of monodentate surface complexes; this implies the use of Equations (A5) and (A8) in Appendix 1 for 2,4-D and clofencet, and Equations (A6) and (A9) for salicylic acid, if formation of adsorbed charged complexes are neglected as a first approximation.

3 Surface ionization of oxides is described with mean equilibrium constants calculated from published data. Values of the mean intrinsic equilibrium constants were taken as those for aluminium oxides reported by Goldberg & Sposito (1984):

$$\log K^+(\text{int}) = 7.38 \pm 0.61 \quad (8)$$

and

$$\log K^-(\text{int}) = -9.09 \pm 0.68.$$

According to these authors, values for Fe oxides are not statistically different from those of Al oxides. Therefore, these values were used for both gibbsite and goethite.

4 Soil oxides behave as a weighted mixture of goethite and gibbsite according to the additivity approach.

5 Mean specific surface areas of goethite and gibbsite could be estimated from published values and are given in Table 3.

6 The capacitance density is constant and equal to 1.06 F m^{-2}. This value has been shown to be appropriate for describing phosphate adsorption on various oxides because the model is insensitive to this parameter (Goldberg & Sposito, 1984).

Curves are usually fitted to obtain equilibrium constants, but here we calculated their values from adsorbed amounts. A numerical procedure was used to obtain the values of σ that equalized two expressions of the reciprocal of the SOH concentration ($\frac{1}{[SOH]}$)deduced from Equations (A3) and (A8). Then, the concentrations of the various species were calculated. This led to the following relationship linking the surface electric charge and the pH:

$$\sigma = 0.258 - 0.0314\ \text{pH}, \quad (9)$$

where σ is expressed in mol kg^{-1}.

Estimated [SOH] concentrations allow the calculation of K_L^1(int) values from the experimentally derived adsorbed amounts [SL], from Equations (A5) and (A11) and the mass balance equation for the organic acid:

$$C_T = [SL] + [HL] + [L^-]. \quad (10)$$

Amounts of goethite and gibbsite for each soil used in the calculation are listed in Table 2, and the specific surface areas and the maximum surface charge densities are given in Table 3. Calculations revealed a linear relationship between the logarithm of the intrinsic equilibrium constant (K_L^1(int)) and the surface electric charge:

$$\log K_L^1(\text{int}) = \log K_L^1(\text{int})o - b\sigma, \quad (11)$$

where σ is a function of pH given by Equation (9).

Estimated values for log K_L^1(int)o, b and their associated estimated errors are provided in Table 4. If the constant capacitance model applies under the assumptions discussed above then the intrinsic equilibrium constant should be

Table 3 Maximum site densities (from Sposito, 1984) and mean specific surface area of goethite and gibbsite

	Number of OH_2^+ groups		Number of O^- groups	
	mol m^{-2}	mol kg^{-1}	mol m^{-2}	mol kg^{-1}
Goethite	4.4×10^{-6}	0.257	6.7×10^{-6}	0.397
Gibbsite	2.8×10^{-6}	0.227	5.6×10^{-6}	0.454

Mean specific surface area for goethite = 59 $m^2\ g^{-1}$.
Mean specific surface area for gibbsite = 81 $m^2\ g^{-1}$.
Mean values are obtained from published data given in Table 2 of Appendix 3.

independent of the surface electric charge and thus, of the pH. The dependence observed between the intrinsic equilibrium constants and pH can be due either to a deficiency of the theoretical model used or to the consequences of the assumptions made for its application. Although the ability of the constant capacitance model to describe numerically anion adsorption has been essentially demonstrated for inorganic substances and less frequently for organic substances (Goldberg, 1992), its application in the present case needs discussing. With regard to the model formulation itself, the validity of the linear relationship between Ψ and σ has been questioned, making the CC model inappropriate for describing adsorption for systems with low values of the ionic strength (Lützenkirchen, 1999). With regard to molecular mechanisms involved in the adsorption, we have considered only adsorption reactions leading to monodentate surface complexes. The hypothesis is obviously valid for 2,4-D and clofencet, which are monoprotic acids, but it remains questionable for salicylic acid. This last

Table 4 Relationship between the intrinsic equilibrium constant (K_L^1(int)) and the surface electric charge (σ) obtained with the constant capacitance model (CC model): $\log K_L^1(\text{int}) = \log K_L^1(\text{int})\text{o} - b\ \sigma$; $s_{\log K(\text{int})\text{o}}$ and s_b are the calculated standard errors

Soil	$\log K_L^1$(int)o	$s_{\log K(\text{int})}$	b	s_b	R^2 (0.05)
2,4-D					
Fertans	6.88	0.07	20.1	0.9	0.9803
Villeroy	7.44	0.05	25.7	0.7	0.9816
Maves	7.60	0.30	24.1	3.0	0.8990
Ouénarou	5.60	0.03	13.4	0.3	0.9941
Maré	6.42	0.04	17.1	0.6	0.9916
Clofencet					
Fertans	7.10	0.03	12.4	0.5	0.9572
Villeroy	7.12	0.04	16.2	0.5	0.9881
Maves	7.60	0.05	12.2	0.8	0.9376
Ouénarou	5.86	0.04	7.8	0.5	0.9457
Maré	6.16	0.02	14.2	0.4	0.9897
Salicylic acid					
Fertans	7.6	0.1	26.7	1.3	0.9784
Villeroy	7.2	0.2	17	3	0.8316
Maves	7.2	0.2	16	2	0.8691
Ouénarou	8.5	0.7	33	6	0.8431
Maré	6.2	0.3	14	5	0.6088

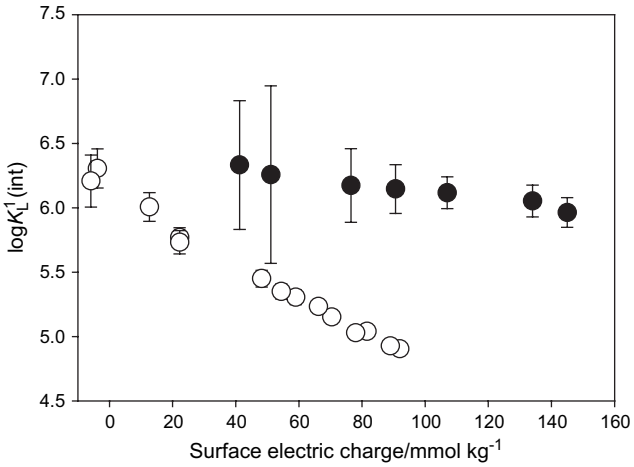

Figure 1 Variation of the logarithm of the intrinsic equilibrium (K_L^1(int)) with the surface electric charge for Clofencet; pure oxide (γ-Al_2O_3), ●; Maré soil, ○. The bars indicate the confidence limits (0.05).

compound can be sorbed through bidentate complex on goethite (Evanko & Dzombak, 1999). However, consideration of the bidendate nature of the complexes would not be required in practice to replicate experimental data (Goldberg, 1992). Another point to consider for salicylic acid is that it may be partly adsorbed through charged surface complexes, as described by Reaction (7). This binding process was not accounted for in our approach, and we have therefore neglected the adsorption of salicylic acid, which takes place from pH = 6 and reaches a maximum around pH = 8, as calculated for γ-Al_2O_3 (Kummert & Stumm, 1980) and deduced from calorimetric measurements (Benoit *et al.*, 1993).

Another factor explaining the relationship obtained between the intrinsic equilibrium constants and the pH is that the CC model is meant to describe only adsorption on oxide surfaces or equivalent surfaces such as those of crystal edges of clays. The CC model is not suited to account for interactions of organic acids with organic matter because specific protonation-dissociation values are not currently available for it (Goldberg *et al.*, 2000). Note that the issue of organic matter is of wider relevance because this constituent has conflicting effects that are likely to interfere in the adsorption process, beyond the protonation and dissociation of organic groups. These include a positive role on adsorption through hydrophobic and polar interactions, which are likely to affect both the ionized and non-ionized forms of organic acids, and a negative role by competing specifically with anions for adsorption on positive electric surface sites (Gustafsson, 2001), through repulsion of anions from ionized organic groups and through physical coating of mineral surfaces. The latter effect, which limits the interaction of organic acids with organic matter, is also invoked for the 'umbrella effect', which limits the number of adsorption sites accessible to ligands (Kovacevic *et al.*, 1998). These various interacting effects have not yet been introduced into adsorption

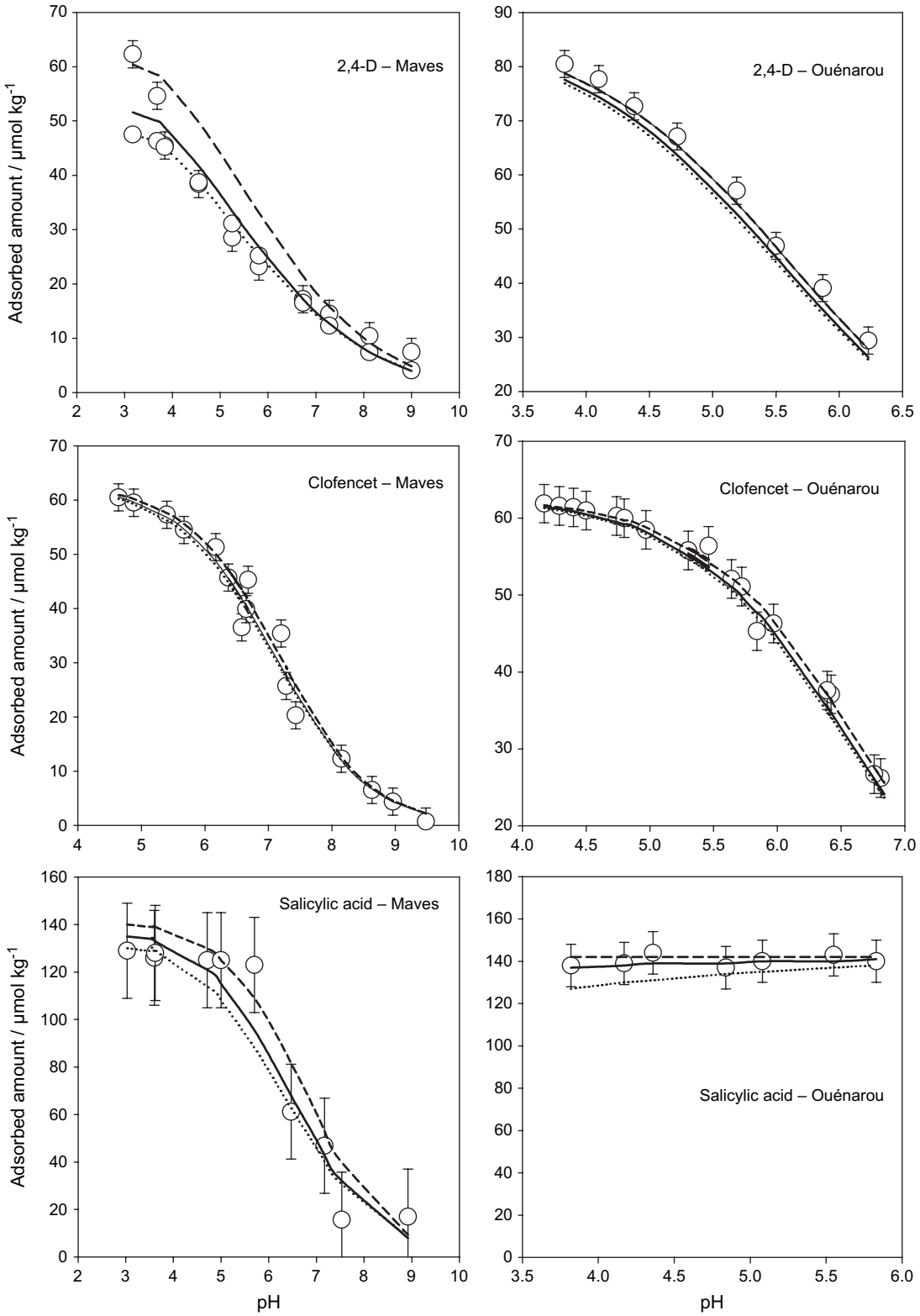

Figure 2 Variations in adsorbed amounts with pH for 2,4-D, Clofencet and salicylic acid on the Maves and Ouénarou soils. The round symbols represent the experimental data while the line in full corresponds to simulations obtained using the CC model. The bars represent an estimation of the confidence limit of experimental data (0.05) and the dotted and dashed lines represent an estimation of the confidence limit (0.05) of simulations.

models. The potential important role played by organic matter in the adsorption of organic acids can be illustrated through data for the Maré soil, which contains much Al oxide and the composition of which is close to pure alumina. Figure 1 compares the variation of log K_L^1 (int) against σ for the Maré soil and a synthetic alumina material. The observed difference between the slopes of the two curves may reflect the effect of organic matter on adsorption and could explain the variation of log K_L^1 (int) with pH noted for the five soils.

Differences in values of K_L^1(int)o between compounds were of the same order of magnitude as differences between soils (Table 4). This accords with a limited influence of the molecular structure on the adsorption of small organic molecules, as noted by Evanko & Dzombak (1999). Few studies of the adsorption of organic compounds allow critical evaluation of the values we obtained. Kummert & Stumm (1980) obtained a value of log K_L^1(int)o = 6 for the adsorption of the salicylate ion on γ-Al_2O_3, a value that is similar to the one we obtained for salicylate on the Maré soil, characterized by a large content of gibbsite (Table 4). The value obtained for the adsorption of salicylic acid on the Ouénarou soil (characterized by a large content of goethite) (Table 4) also compares favourably with the value of log K_L^1(int)o = 8.5 reported for the adsorption of salicylic acid on goethite by Evanko & Dzombak (1999).

Simulation of the experimental data using K_L^1(int) values

We predicted adsorbed amounts of the three organic acids in the five soils using Equations (A5) and (10) with parameter values given in Table 4 and protonation dissociation equilibrium characteristics given by Equation (8). Representative examples of the comparison between experimental and simulated adsorbed amounts are displayed in Figure 2. We estimated the minimum and maximum adsorbed amounts with the estimated errors given in Table 4, which provide an indication of the uncertainty domain to be expected on the predictions. Table 5 lists values for three statistical tests that can be used to assess numerically the goodness-of-fit between observed and predicted values represented graphically on Figure 2. The goodness-of-fit indices showed a good fit of the model predictions to the observed data. We emphasize that the favourable comparison observed does not give any indication of the predictive ability of the model as predictions were partly based on the data themselves. The comparison therefore demonstrates only that the model and its associated parameter values can provide the correct shape of the variation of adsorption with pH and that the experimental data can be numerically described on the basis of Equation (11).

Given the limitations reported above, the ability of the model to provide suitable predictions for experimental data was further assessed by predicting adsorption isotherms for clofencet on two of the soils considered (Maves and Villeroy). Parameters for clofencet and the two Cambisols (Table 4) were used to calculate adsorption isotherms at a range of pH. Figure 3 presents results obtained at pH 5 and pH 7. Similar results were obtained at other pH (data not shown). Visual assessments and goodness-of-fit tests generally indicated a fairly good fit to the measured isotherm data, except for the soil Maves at pH > 7.0, probably because of large experimental errors when adsorbed amounts are very small. This demonstrates that the CC model and the additivity approach have an overall good potential for predicting adsorption isotherms of organic acids at varied pH.

Table 5 Statistical tests for the CC model applied to adsorption of the three organic acids on the five selected soils; *n* is the number of data points in the adsorbed amount versus pH curve. ME = model efficiency, TE = total error, SRMSE = scaled root mean square error (definitions are given in Appendix 4)

Soil	*n*	TE	SRMSE	ME
2,4-D				
Fertans	11	0.065	0.104	0.870
Villeroy	10	0.151	0.114	0.840
Maves	10	0.127	0.154	0.930
Ouénarou	8	0.054	0.056	0.970
Maré	8	0.017	0.021	0.986
Clofencet				
Fertans	28	0.061	0.082	0.969
Villeroy	16	0.076	0.091	0.983
Maves	16	0.053	0.081	0.980
Ouénarou	17	0.023	0.028	0.986
Maré	15	0.031	0.037	0.992
Salicylic acid				
Fertans	11	0.077	0.083	–1.4
Villeroy	7	0.171	0.193	0.676
Maves	10	0.108	0.132	0.983
Ouénarou	7	0.013	0.017	–0.08
Maré	8	0.100	0.111	0.694

We tested the model further by attempting to simulate a set of adsorption coefficients (K_d) measured for the three organic acids on seven Cambisols and six Ferralsols at their native pH (Dubus *et al.*, 2001). We took log K_L^1(int)o and *b*-values as follows. For Cambisols, the average value for the Fertans, Villeroy and Maves soils (Table 4) was used. For Ferralsols, we distinguished between compounds. For 2,4-D and clofencet, we used mean values of log K_L^1(int)o and *b* calculated from the combined Ouénarou and Maré data (Table 4), while parameters corresponding to the soils of Ouénarou and Maré were used separately for salicylic acid. For Cambisols, the adsorption of 2,4-D and clofencet was predicted adequately except for the adsorption of 2,4-D on two soils for which adsorbed amounts were overestimated (Figure 4). In contrast, the adsorption of salicylic acid on Cambisols was underestimated. We attribute the underestimation to the fact that the CC model does not describe the adsorption on organic matter. For Oxisols, a reasonable fit was obtained for clofencet and salicylic acid but only partly for 2,4-D (Figure 4). Experimental data for salicylic acid were best simulated with parameters corresponding to goethite.

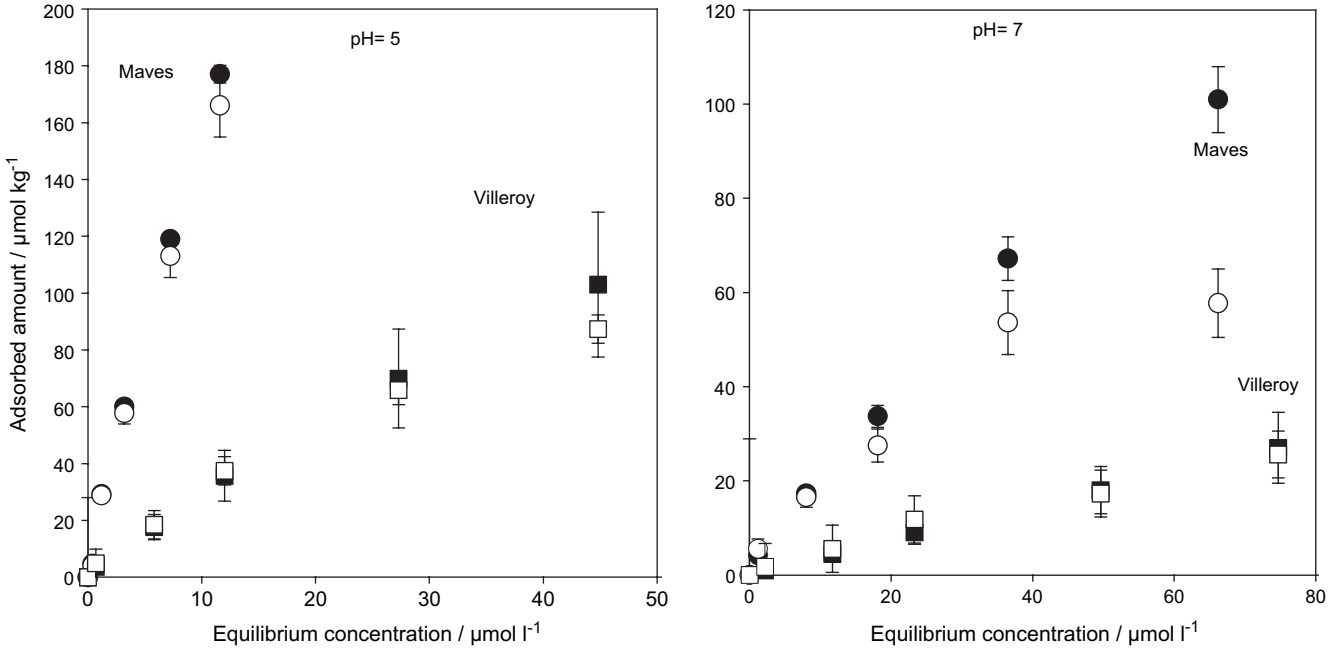

Figure 3 Adsorption isotherms of Clofencet on the Maves and Villeroy soils. The open symbols represent the experimental adsorbed amounts. The filled symbols correspond to predictions obtained using the CC model. The bars indicate the confidence limits (0.05).

Overall, the two evaluation exercises show that the CC model can provide valuable insights into the adsorption of organic acids and can give, at least, a first approximation of sorption data based on the literature and few experimental data.

Theory and application of the Stern variable surface charge–variable surface potential model (VSC-VSP model)

Model theory

The VSC-VSP model is an extension of the Stern model, which describes the distribution of ions at interfaces between electrified solid surfaces and ionic solutions. It was further developed to account for the charging process and anion adsorption by Barrow *et al.* (1980), Barrow (1983) and Barrow & Bowden (1987). In this model, ions are distributed among four layers so that the model is also known as the 'four-layer model' and sometimes as the 'objective model' (Sposito, 1984). Figure 5 represents schematically the surface solution interface of the VSC-VSP model. Protons, hydroxyl ions and strongly adsorbed anions and cations form inner-sphere surface complexes, while loosely adsorbed ions form outer-sphere complexes. Protons and hydroxyl ions lie on a plane very close to the solid surface (plane 's'). Some cations and anions of the background electrolyte forming outer-sphere complexes are assumed to be in a plane some distance from the surface (plane 'β'). Other species are assumed to be distributed in the diffuse layer, the charge of which is localized in a plane at a greater distance from the surface (plane 'd'). Adsorbed anions forming inner-sphere complexes are situated between planes 's' and 'β' (plane 'a'), but their actual location is not always clearly defined, even by the authors of the model, who consider that these anions could be in several planes.

The model is formulated with several equations relating the electric potential and the electric charges and expressing electric charges in the various planes. They are given in Appendix 2.

Determination of K_i *values*

As for the CC model, we selected parameter values from the literature and used them to estimate the binding constants of specifically adsorbed ions. This implies that the exercise gives a general evaluation of the potential of the VSC-VSP model to describe the effects of pH on adsorption. The application of the model was based on the procedures reported by Barrow *et al.* (1980). The electric potential at plane 's' (Ψ_s) was first varied to obtain two identical estimations of σ_s, one provided by Equation (B4) and another one by Equation (B8) in Appendix 2. We used a numerical procedure to solve Equations (B4) to (B8), thereby providing estimates of electric charges and potentials for given pH and background electrolyte concentrations. As σ_a is smaller than σ_s (1–3%), we neglected it in our calculations. This approximates to considering only the planes 's' and 'β' for the calculation of other charges and potentials. Once Ψ_a was determined, we calculated K_i values using Equation (B6), assuming the activities

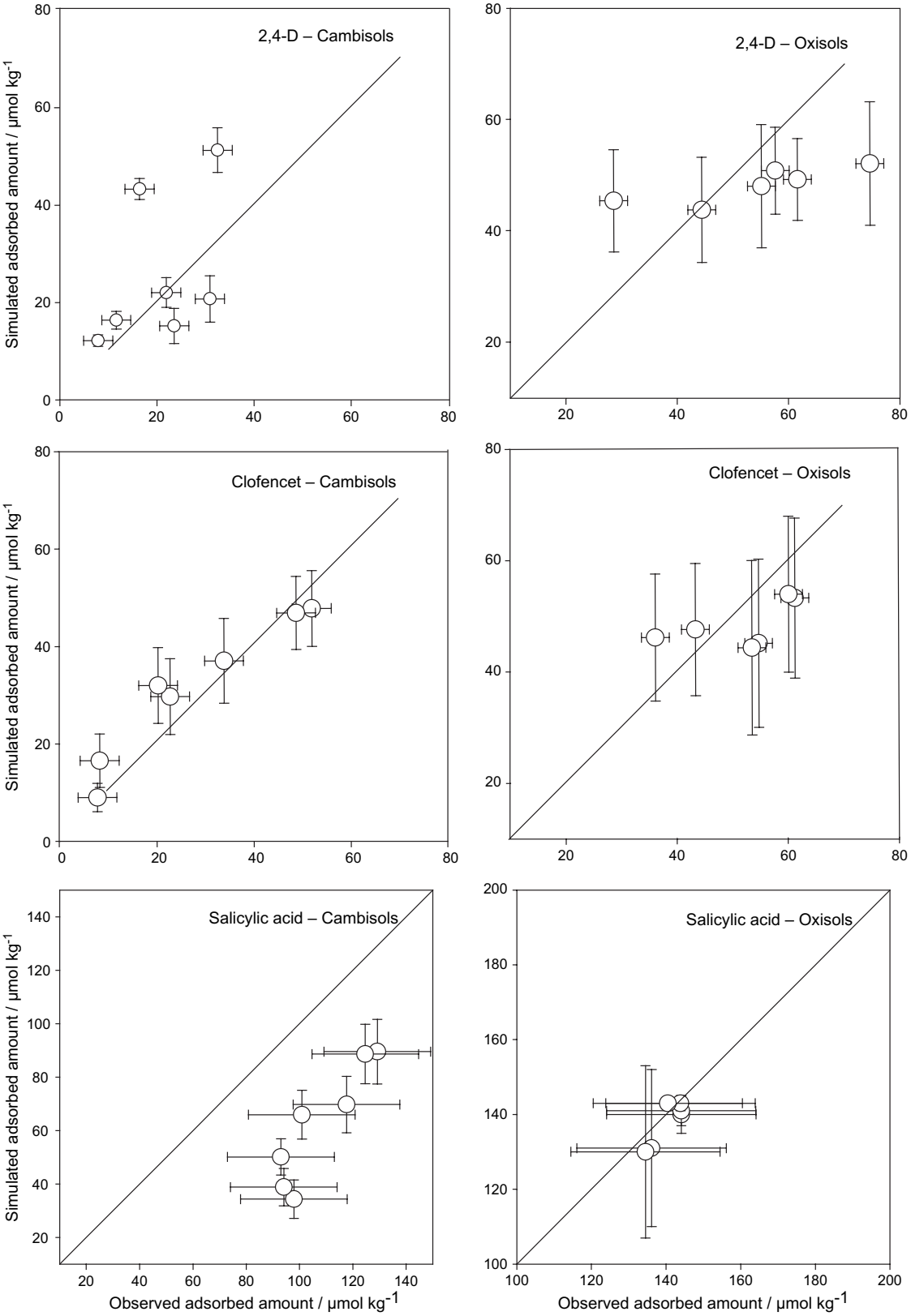

Figure 4 Comparison between observed and calculated adsorbed amounts of the three organic acids on several Cambisols and Ferralsols at their native soil pH. The bars indicate the confidence limits (0.05). Experimental data are given in Dubus *et al.* (2001).

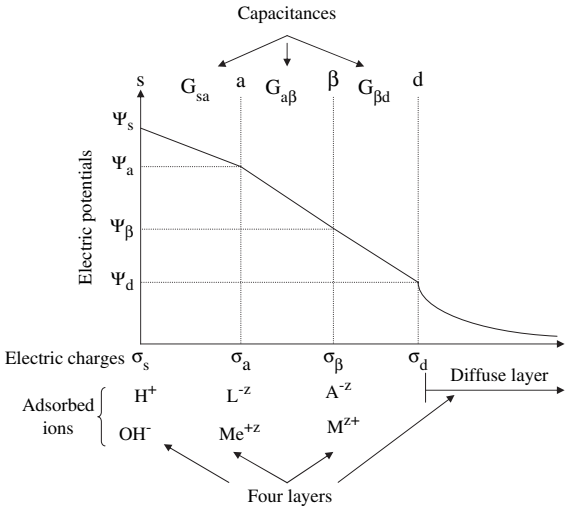

Figure 5 Schematic diagram of the surface–solution interface for the VSC-VSP model.

of the adsorbed molecules could be replaced by their concentrations in the calculations. Estimations of the errors on K_i values were obtained from the experimental errors on adsorbed amounts.

The model parameterization procedure requires that values are assigned to the parameters K and G appearing in Equations (B1) to (B6). These were taken as values established for the adsorption of inorganic anions on a suspension of goethite in $CaCl_2$ ($K_H = 30.8 \times 10^6$ litres mol^{-1}, $K_{OH} = 0.392 \times 10^6$ litres mol^{-1}, $K_{cat} = 2.12$ litres mol^{-1}, $K_{an} = 0.38$ litres mol^{-1}, $G_{s\beta} = 15.4 \times 10^{-6}$ mol V^{-1} m^{-2} and $G_{\beta d} = 40 \times 10^{-6}$ mol V^{-1} m^{-2}; Barrow *et al.*, 1980). With regard to the selection of values for the adsorbed densities of proton hydroxyl groups, N_S and N_T, we assumed that the properties of all oxides were similar with regard to ion adsorption and that they may be described by the mean values reported in Table 3. In accordance with procedures used for the CC model, an amount of 'equivalent' oxide was calculated on the basis of the mineralogical composition of the soils. The adsorbed density of specifically adsorbed ions N_T was taken as a weight mean of several published values (2.3×10^{-6} mol m^{-2}, Appendix 3, Table 2). As noted above, the exact location of the plane 'a' is subject to debate and deriving a value for the potential Ψ_a is therefore problematic. We reviewed critically the literature with regard to this particular aspect, and following the work from Barrow and colleagues (Barrow *et al.*, 1980; Barrow, 1983) we considered that plane 'a' is between planes 's' and 'β', and gets closer to plane 's' as the interactions with the surface become stronger. Values of Ψ_a obtained were generally close or equal to those of Ψ_β. In the pH range of the experimental study, Ψ_a values corresponding to the less variable K_i values appeared to be linear functions of pH (Table 6). The observation accords with that made for the complexation constant K_L^1(int) of the CC model, which we attributed to the ionization of the soil organic matter.

Simulation of the experimental data using K_i values

Values of K_i obtained by the procedure described above were used to predict the experimental data for 2,4-D, clofencet and salicylic acid, which were already used as part of the evaluation of the CC model. We obtained predictions for adsorbed amounts using Equation (B6) together with the mass balance equation, Equation (10). Representative results for the variation of adsorbed amounts with pH are shown in Figure 6. The figure and goodness-of-fit tests for the three compounds show that the shape of the variation of the adsorbed amount as a function of pH was generally well described except for salicylic acid. We tried to improve the simulations by considering the bivalent nature of this compound, but this did not improve the overall goodness of fit.

As for the CC model, adsorption isotherms for clofencet on two soils (Villeroy and Maves) were predicted at various pH. Figure 7 presents a comparison between measured and predicted isotherms at pH 5 and pH 7. This figure, together with goodness-of-fit tests (data not shown) shows that isotherms are generally well described, except for the soil Maves at pH 7. Also, in common with the approach adopted for the CC model, the VSC-VSP model was tested by prediction of the magnitude of adsorption in Cambisols and Ferralsols at their native pH. The application of the model relied on the use of mean values

Table 6 Relationship between the potential Ψ_a (V) and pH obtained with the VSC-VSP model. $\Psi_a = (a \pm s_a) - (b \pm s_b)$pH and mean values of the binding constant, $'K_i \pm {}^S K_i$ (± estimated error)

	K_i / litre mol^{-1}	$^S K_i$ / litre mol^{-1}	a	s_a	b	s_b	R^2 (0.05)
2,4-D							
Fertans	20	6	0.19	0.02	0.022	0.004	0.7819
Villeroy	30	6	0.10	0.006	0.009	0.0009	0.9455
Maves	38	19	0.16	0.01	0.019	0.002	0.9139
Ouénarou	1.4	0.1	0.265	0.004	0.032	0.008	0.9963
Maré	4	3	0.25	0.02	0.031	0.003	0.9645
Clofencet							
Fertans	73	12	0.259	0.007	0.032	0.001	0.9804
Villeroy	49	13	0.210	0.009	0.025	0.001	0.9584
Maves	182	60	0.26	0.01	0.033	0.002	0.9756
Ouénarou	5.6	0.6	0.333	0.009	0.043	0.002	0.9756
Maré	2.8	0.8	0.20	0.02	0.022	0.003	0.7970
Salicylic acid							
Fertans	77	34	0.14	0.02	0.015	0.003	0.7564
Villeroy	53	35	0.412	0.002	0.0555	0.0003	0.9998
Maves	113	34	0.19	0.01	0.023	0.002	0.9511
Ouénarou	3	3	0.408	0.004	0.0543	0.0007	0.9990
Maré	4	4	0.35	0.06	0.045	0.009	0.8625

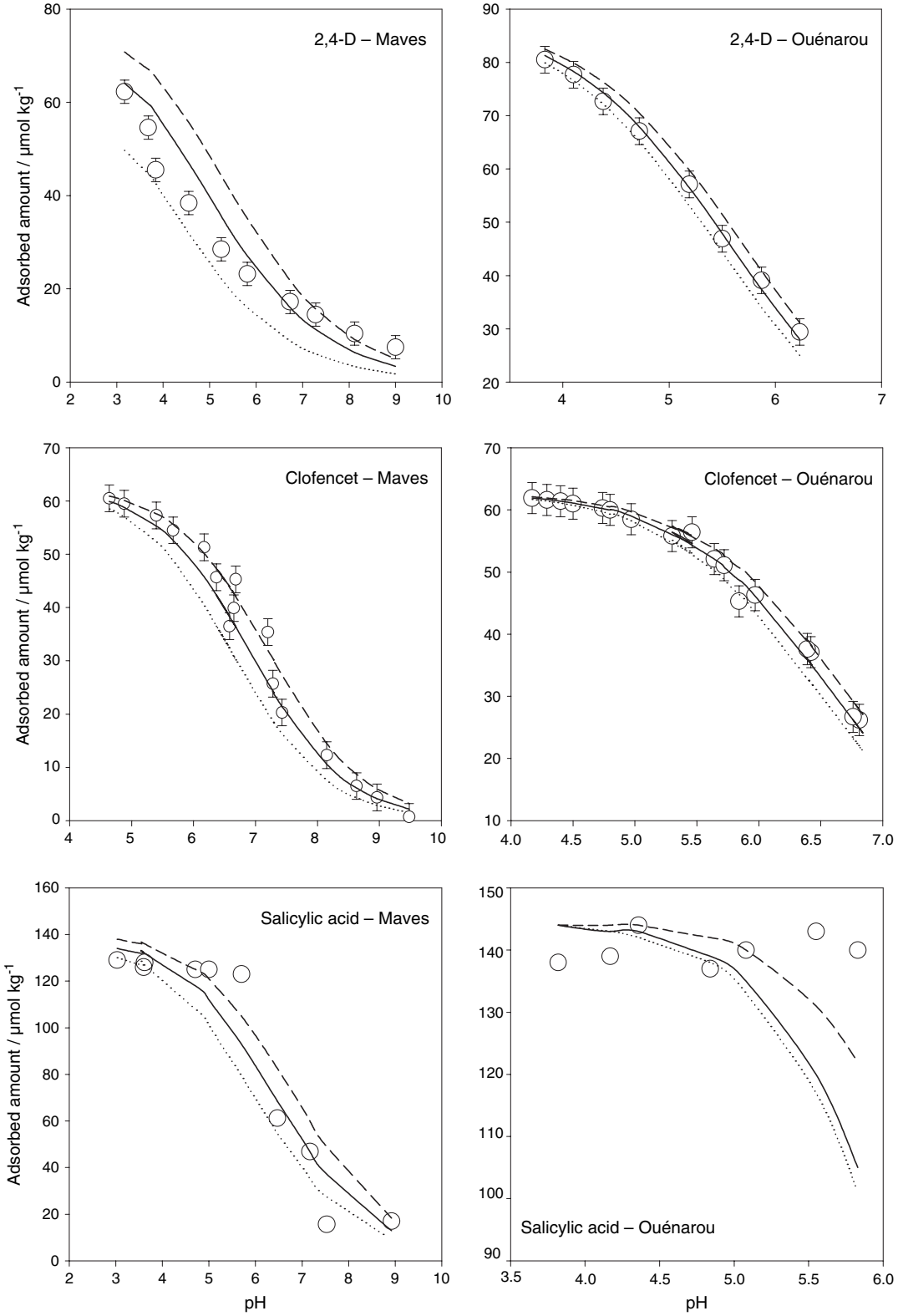

Figure 6 Variations in adsorbed amounts with pH for 2,4-D, Clofencet and salicylic acid on the Maves and Ouénarou soils. The round symbols represent the experimental data while the line in full corresponds to simulations obtained using the VSC VSP model. The bars represent an estimation of the confidence limit of experimental data (0.05) and the dotted and dashed lines represent an estimation of the confidence limit (0.05) of simulations.

for K_i values and the relationship between Ψ_a and pH. For Cambisols, values were taken as the mean of values obtained for Fertans, Villeroy and Maves ($K_i = 28 \pm 10$ litres mol^{-1}, $\Psi_a = (0.15–0.17\ \text{pH})$ V, $\Delta\Psi_a = 0.008$ V where $\Delta\Psi_a$ represents an estimation of the mean uncertainty on Ψ_a in the experimental pH range). For Ferralsols, values were taken as the mean of values obtained for Ouénarou and Maré ($K_i = 2.7 \pm 1.6$ litres mol^{-1}, $\Psi_a = (0.26–0.315\ \text{pH})$ V and $\Delta\Psi_a = 0.006$ V). Standard deviations are fairly large because of an amplification effect of the numerical procedure. The use of mean values implies that anion surface interactions and the variation of Ψ_a with pH are the same for all soils within a group. The same conclusions as for the CC model can be drawn from the comparison between measured and calculated adsorbed amounts.

Concluding remarks

A comparison of the performance of the two surface complexation models with regard to their ability to represent the variation of adsorbed amounts of three organic acids with pH is presented in Table 7, which lists mean values of goodness-of-fit tests. Overall, the adsorption of 2,4-D and clofencet was better described than the adsorption of salicylic acid. The CC model resulted in the best simulation for the three organic acids, although the VSC VSP model provided good simulations of the clofencet data. Considering the assumptions that had to be made to apply the two models, in particular with regard to the use of literature values for several of the parameters, we conclude that the two models performed generally well. The CC and the VSC VSP models were found to be roughly equivalent for predicting adsorbed amounts on the soils we investigated. The poorer description of the salicylic data we tentatively attribute to the fact that the models considered only monodentate surface complexes.

The modelling showed that the adsorption of organic acids in soils could be adequately simulated on the basis of an adsorption on oxide and hydroxide surfaces by a combination of pure mineral properties. Although this is of particular interest for prediction purposes, the approach is still somewhat limited from a mechanistic point of view. The set of soils used was too small to allow the construction of a mechanistically based tool for predicting adsorption. The influence of 2:1 phyllosilicates and that of the organic matter on adsorption are not accounted for in the models. A modification of the models to account for their effects would be likely to result in a further improvement of the simulations. For organic matter, the effects that could be described include the contribution of ionized carboxylic groups to the surface electric potential and the competition for adsorption sites provided by acidic groups of the organic matter. This latter effect would be important because organic acids are adsorbed mainly through ligand exchange and provide a direct and effective competition to other acids, whether they are inorganic or organic. The soil organic matter could also be involved in the adsorption of organic acids by hydrophobic interactions. For ionized compounds, these interactions could result in a modification of the surface electric charge. We know, however, that the adsorption of non-ionized compounds is intimately linked to

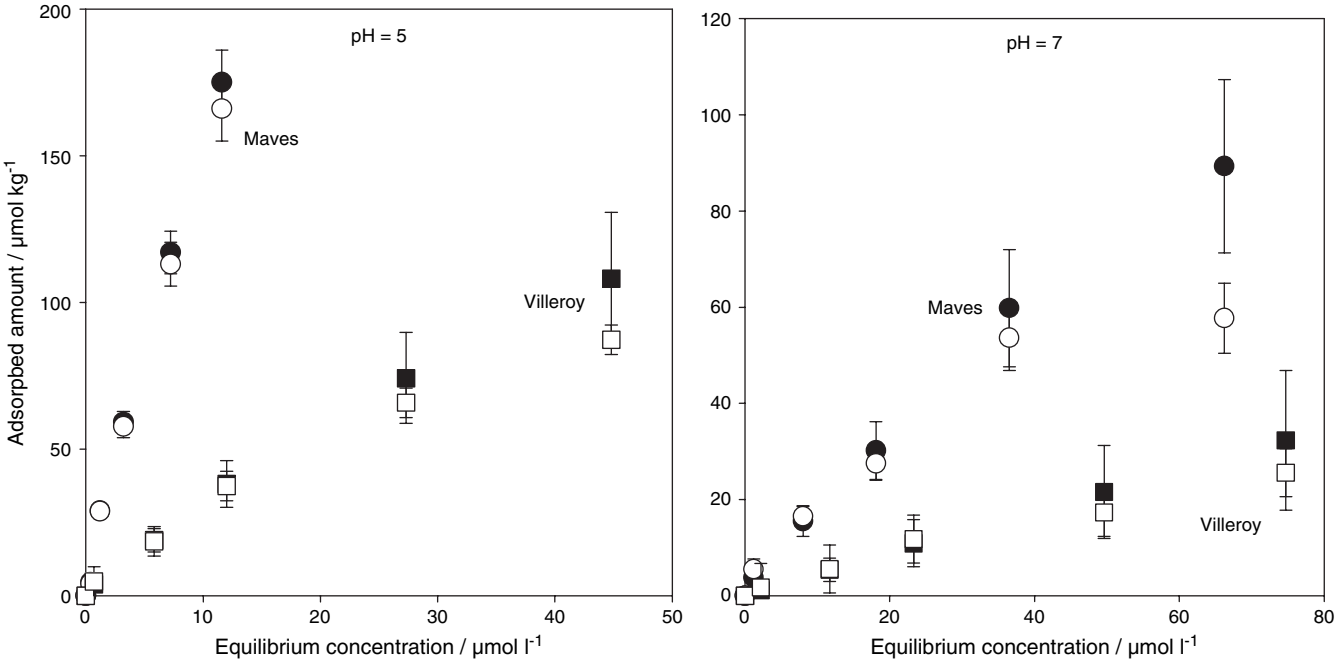

Figure 7 Adsorption isotherms of Clofencet on the Maves and Villeroy soils. The open symbols represent the experimental adsorbed amounts. The filled symbols correspond to predictions obtained using the VSC-VSP model. The bars indicate the confidence limits (0.05).

Table 7 Goodness-of-fit scores obtained for the CC and VSC VSP models for the prediction of the relationship between adsorbed amounts and pH for the three organic acids in the five soils. Definitions of statistical tests, TE, SRMSE and ME are given in Appendix 4

	CC model			VSC VSP model		
	TE	SRMSE	ME	TE	SRMSE	ME
2,4-D	0.08	0.09	0.92	0.12	0.14	0.78
Clofencet	0.05	0.06	0.98	0.07	0.09	0.96
Salicylic acid	0.09	0.11	0.17	0.13	0.17	–10.7

soil organic matter. In the case of the three ionizable organic compounds we consider, this would imply that the compounds remain partly non-ionized at the interface between solid and liquid in the range of pH 4–9. This could be envisaged if the organic acids had a greater pK_a value near adsorbing surfaces than in solution, or they experience a surface pH much lower than the pH in solution. The latter hypothesis was suggested by Farmer & Aochi (1974) and Nicholls & Evans (1991), but the former has received little attention. The reasons for low pH close to interacting surfaces is well understood for weakly hydrated clays, but those for well-hydrated soils are not yet clearly understood for materials such as soils and sediments. An improved knowledge of the physicochemical properties of systems containing water, mineral materials and organic matter would therefore improve the description of organic acid adsorption.

Acknowledgements

The experimental data used in the modelling was initially obtained as part of a study funded by Monsanto.

References

Barrow, N.J. 1983. A mechanistic model for describing the sorption and desorption of phosphate by soil. *Journal of Soil Science*, **34,** 733–750.

Barrow, N.J. 1999. The four laws of soil chemistry: the Leeper lecture 1998. *Australian Journal of Soil Research*, **37,** 787–829.

Barrow, N.J. & Bowden, J.W. 1987. A comparison of models for describing the adsorption of anions on a variable charge mineral surface. *Journal of Colloid and Interface Science*, **119,** 236–250.

Barrow, N.J., Bowden, J.W., Posner, A.M. & Quirk, J.P. 1980. An objective method for fitting models of ion adsorption on variable charge surfaces. *Australian Journal of Soil Research*, **18,** 37–47.

Barrow, N.J., Brümmer, G.W. & Strauss, R. 1993. Effects of surface heterogeneity on ion adsorption by metal oxides and by soils. *Langmuir*, **9,** 2606–2611.

Becquer, T., Pétard, J., Duwig, C., Bourdon, E., Moreau, R. & Herbillon, A.J. 2001. Mineralogical, chemical and charge properties of Geric Ferralsols from New Caledonia. *Geoderma*, **103,** 291–306.

Benoit, P., Hering, J.G. & Stumm, W. 1993. Comparative study of the adsorption of organic ligands on aluminum oxide by titration calorimetry. *Applied Geochemistry*, **8,** 127–139.

Cornell, R.M. & Schindler, P.W. 1980. Infrared study of the adsorption of hydroxycarboxylic acids on α-FeOOH and amorphous Fe (III) hydroxide. *Colloid and Polymer Science*, **258,** 1171–1175.

Davis, J.A., Coston, J.A., Kent, D.B. & Fuller, C.C. 1998. Application of the surface complexation concept to complex mineral assemblages. *Environmental Science and Technology*, **32,** 2820–2828.

Dubus, I.G., Barriuso, E. & Calvet, R. 2001. Sorption of weak organic acids in soils: clofencet, 2,4-D and salicylic acid. *Chemosphere*, **45,** 767–774.

Duchaufour, P. 1995. *Pédologie*. Masson, Paris.

Evanko, C.R. & Dzombak, D.A. 1999. Surface complexation modelling of organic acid sorption to goethite. *Journal of Colloid and Interface Science*, **214,** 189–206.

Farmer, W.J. & Aochi, Y. 1974. Picloram sorption by soils. *Soil Science Society of America Proceedings*, **38,** 418–423.

Goldberg, S. 1992. Use of surface complexation models in soil chemical systems. In: *Advances in Agronomy* (ed. D.L. Sparks), pp. 233–329. Academic Press, New York.

Goldberg, S. 2005. Inconsistency in the triple layer model description of ionic strength dependent boron adsorption. *Journal of Colloid and Interface Science*, **285,** 509–517.

Goldberg, S., Lesch, S.M. & Suarez, D.L. 2000. Predicting boron adsorption by soils using soil chemical parameters in the constant capacitance model. *Soil Science Society of America Journal*, **64,** 1356–1363.

Goldberg, S. & Sposito, G. 1984. A chemical model of phosphate adsorption by soils. I. Reference oxide minerals. *Soil Science Society of America Journal*, **48,** 772–778.

Gustafsson, J.P. 2001. Modelling competitive anion adsorption on oxide minerals and an allophane-containing soil. *European Journal of Soil Science*, **52,** 639–653.

Hingston, F.J. 1981. A review of anion adsorption. In: *Adsorption of Inorganics at Solid–Liquid Interfaces* (eds M.A. Anderson & A.J. Rubin), pp. 51–91. Ann Arbor Science Publishers, Ann Arbor, Michigan.

Horanyi, G. 2002. Specific adsorption of simple organic acids on metal (hydr) oxides: a radiotracer approach. *Journal of Colloid and Interface Science*, **254,** 214–221.

Jeanroy, E. 1983. *Diagnostic des formes du fer dans les pédogenèses tempérées. Evaluation par les réactifs chimiques d'extraction et apports de la spectrométrie Mössbauer*. Thèse de doctorat. Université Nancy I, Nancy, France.

Kovacevic, D., Kobal, I. & Kallay, N. 1998. Adsorption of organic acids on metal oxides. The umbrella effect. *Croatica Chemica Acta*, **71,** 1139–1153.

Kubicki, J.D., Itoh, M.J., Schroeter, L.M. & Apitz, S.E. 1997. Bonding mechanisms of salicylic acid adsorbed onto illite clay: an ATR-FTIR and molecular orbital study. *Environmental Science and Technology*, **31,** 1151–1156.

Kummert, R. & Stumm, W. 1980. The surface complexation of organic acids on hydrous γ-Al_2O_3. *Journal of Colloid and Interface Science*, **75,** 373–385.

Lützenkirchen, J. 1999. The constant capacitance model and variable ionic strength: an evaluation of possible applications and applicability. *Journal of Colloid and Interface Science*, **217,** 8–18.

Mehra, O.P. & Jackson, M.L. 1960. Iron oxide removal from soils and clays by dithionite-citrate systems buffered with sodium bicarbonate. *Clays and Clay Minerals*, **7,** 317–327.

Nicholls, P.H. & Evans, A.A. 1991. Sorption of ionisable organic compounds by field soils. Part 1. Acids. *Pesticide Science*, **33,** 319–330.

Parfitt, R.L. & Childs, C.W. 1988. Estimation of forms of Fe and Al: a review, and analysis of contrasting soils by dissolution and Moessbauer methods. *Australian Journal of Soil Research*, **26,** 121–144.

Parfitt, R.L., Farmer, V.C. & Russel, J.D. 1977a. Adsorption on hydrous oxides. I. Oxalate and benzoate on goethite. *Journal of Soil Science*, **28,** 29–39.

Parfitt, R.L., Fraser, A.R., Russel, J.D. & Farmer, V.C. 1977b. Adsorption on hydrous oxides. II. Oxalate, benzoate and phosphate on gibbsite. *Journal of Soil Science*, **28,** 40–47.

Schwertmann, U. & Latham, M. 1986. Properties of iron oxides in some New Caledonian Oxisols. *Geoderma*, **39,** 105–123.

Sposito, G. 1984. *The Surface Chemistry of Soils*. Oxford University Press, New York.

Tadanier, C.J. & Eick, M.J. 2002. Formulating the charge distribution multisite surface complexation model. *Soil Science Society of America Journal*, **66,** 1505–1517.

Taubaso, C., Dos Santos Afonso, M. & Torres Sánchez, R.M. 2004. Modelling soil surface charge density using mineral composition. *Geoderma*, **121,** 123–133.

Westall, J. & Hohl, H. 1980. A comparison of electrostatic models for the oxide/solution interface. *Advances in Colloid Interface Science*, **12,** 265–294.

Zuyi, T., Taiwei, C. & Lei Weijuan 2000. On the application of surface complexation models to ionic adsorption. *Journal of Colloid and Interface Science*, **232,** 174–177.

Additional references

Bowden, J.W., Nagarajah, S., Barrow, N.J., Posner, A.M. & Quirk, J.P. 1980. Describing the adsorption of phosphate, citrate and selenite on a variable-charge mineral surface. *Australian Journal of Soil Research*, **18,** 49–60.

Datta, M. & Kunal Ghosh. 1992. Oxides and hydrous oxides of iron and aluminum: an approach for their isolation from soils and their characteristics as compared with synthetic and natural minerals. *Pedology*, **42,** 297–326.

Goldberg, S. & Glaubig, R.A. 1985. Boron adsorption on aluminum oxide minerals. *Soil Science Society of America Journal*, **49,** 1374–1379.

Goldberg, S. & Glaubig, R.A. 1988. Boron and silicon adsorption on an aluminum oxide. *Soil Science Society of America Journal*, **52,** 87–91.

He, L.M., Zelazny, L.W., Baligar, V.C., Ritchey, K.D. & Martens, D.C. 1997. Ionic strength effects on sulphate and phosphate adsorption on γ-alumina and kaolinite: triple layer model. *Soil Science Society of America Journal*, **91,** 784–793.

Hingston, F.J., Posner, A.M. & Quirk, J.P. 1972. Anion adsorption by goethite and gibbsite. I. The role of the proton in determining adsorption envelopes. *Journal of Soil Science*, **23,** 177–192.

Hohl, H. & Stumm, W. 1976. Interaction of Pb^{2+} with hydrous γ-Al_2O_3. *Journal of Colloid and Interface Science*, **35,** 281–288.

Kavanagh, B.V., Posner, A.M. & Quirk, J.P. 1980. Effect of adsorption of phenoxyacetic acid herbicides on the surface charge of goethite. *Journal of Soil Science*, **31,** 33–39.

Muljadi, D., Posner, A.M. & Quirk, J.P. 1966. The mechanism of phosphate adsorption by kaolinite, gibbsite, and pseudoboehmite. *Journal of Soil Science*, **17,** 212–228.

Parfitt, R.L. 1977. Phosphate adsorption on an oxisol. *Soil Science Society of America Journal*, **41,** 1064–1067.

Parfitt, R.L. 1978. Anion adsorption by soils and soil materials. In: *Advances in Agronomy* (ed. N.C. Brady), pp. 1–50. Academic Press, New York.

Schwertmann, U. & Kämpf, N. 1985. Properties of goethite and hematite in kaolinitic soils of southern and central Brazil. *Soil Science*, **139,** 344–350.

Strauss, R., Brümmer, G.W. & Barrow, N.J. 1997. Effect of crystallinity of goethite. I. Preparation and properties of goethites of differing crystallinity. *European Journal of Soil Science*, **48,** 101–114.

Watson, J.R., Posner, A.M. & Quirk, J.P. 1973. Adsorpion of the herbicide 2,4-D on goethite. *Journal of Soil Science*, **24,** 503–511.

Appendix 1: The constant capacitance model

The relationship between the surface electric charge and the surface electric potential can be written as

$$\sigma = \frac{aG}{F}\Psi, \tag{A1}$$

where s is the surface electric charge (mol kg^{-1}),Ψ is the surface electric potential (V), a is the specific surface area of the adsorbent (m^2 kg^{-1}), G is the capacitance density (F m^{-2}) and F is the Faraday constant ($F = 96\,485$ C mol^{-1}).

The surface electric charge is expressed as

$$\sigma = \sigma_H + \sigma_{is}, \tag{A2}$$

where σ_H is the net proton charge and σ_{is} the charge resulting from the formation of inner-sphere surface complexes. Adsorbed amounts being small, σ_{is} can be neglected and σ is simply given by

$$\sigma = [SOH_2^+] - [SO^-]. \tag{A3}$$

The intrinsic equilibrium constants describing the ionisation of surface OH groups given by reactions (1) and (2) are

$$K_+ (\text{int}) = \frac{[SOH_2^+]}{[SOH][H^+]} \exp\left(\frac{F\Psi}{RT}\right) \tag{A4}$$

and

$$K_- (\text{int}) = \frac{[SO^-][H^+]}{[SOH]} \exp\left(-\frac{F\Psi}{RT}\right),$$

where square brackets represent concentrations (mol $litre^{-1}$) when they are small enough to be used in place of activities.

The intrinsic equilibrium constants describing the formation of surface complexes of the ligand L for Reaction (5) are given as

$$K_L^1(\text{int}) = \frac{[SL]}{[SOH][HL]}, \tag{A5}$$

and as follows for Reactions (6) and (7), respectively,

$$K_L^1(\text{int}) = \frac{[\text{SHL}]}{[\text{SOH}][\text{H}_2\text{L}]}, \tag{A6}$$

$$K_L^1(\text{int}) = \frac{[\text{SL}^-][\text{H}^+]}{[\text{SOH}][\text{H}_2\text{L}]} \exp\left(-\frac{F\psi}{RT}\right). \tag{A7}$$

The mass balance equations of surface OH groups corresponding to reactions (5), (6) and (7), respectively, are

$$[\text{SOH}]_T = [\text{SOH}] + [\text{SOH}_2^+] + [\text{SO}^-] + [\text{SL}], \tag{A8}$$

$$[\text{SOH}]_T = [\text{SOH}] + [\text{SOH}_2^+] + [\text{SO}^-] + [\text{SHL}], \tag{A9}$$

and

$$[\text{SOH}]_T = [\text{SOH}] + [\text{SOH}_2^+] + [\text{SO}^-] + [\text{SL}^{-1}]. \tag{A10}$$

Dissociation reactions must be added to this set of equations. For a monoprotic acid, the equation is

$$\text{HL} \rightleftarrows \text{L}^- + \text{H}^+, \; K_a = \frac{[\text{L}^-][\text{H}^+]}{[\text{HL}]} \tag{A11}$$

where K_a is the dissociation constant of the organic acid.

Appendix 2: The Stern variable surface charge–variable surface potential model

Relations between electric potentials and electric charges are

$$\Psi_s - \Psi_a = \frac{\sigma_s}{G_{sa}}, \tag{B1}$$

$$\Psi_a - \Psi_\beta = \frac{\sigma_s + \sigma_a}{G_{a\beta}}, \tag{B2}$$

$$\Psi_\beta - \Psi_d = \frac{-\sigma_d}{G_{\beta d}}. \tag{B3}$$

Expressions of electric charges are:

$$\sigma_s = \frac{N_s\left\{K_H[\text{H}^+]\exp\left(-\frac{F\Psi_s}{RT}\right) - K_{OH}[\text{OH}^-]\exp\left(\frac{F\Psi_s}{RT}\right)\right\}}{1 + K_H[\text{H}^+]\exp\left(-\frac{F\Psi_s}{RT}\right) + K_{OH}[\text{OH}^-]\exp\left(\frac{F\Psi_s}{RT}\right)}, \tag{B4}$$

$$\sigma_\beta = \frac{N_s\left\{K_{cat}[\text{Cat}^{+z_{cat}}]\exp\left(-\frac{z_{cat}F\Psi_\beta}{RT}\right) - K_{an}[\text{An}^{-z_{an}}]\exp\left(\frac{z_{an}F\Psi_\beta}{RT}\right)\right\}}{1 + K_{cat}[\text{Cat}^{+z_{cat}}]\exp\left(-\frac{z_{cat}F\Psi_\beta}{RT}\right) + K_{an}[\text{An}^{-z_{an}}]\exp\left(\frac{z_{an}F\Psi_\beta}{RT}\right)}, \tag{B5}$$

$$\sigma_a = \frac{N_T \sum_i Z_i K_i a_i \exp\left(-\frac{Z_i F\Psi_a}{RT}\right)}{1 + \sum_i Z_i K_i a_i \exp\left(-\frac{Z_i F\Psi_a}{RT}\right)}, \tag{B6}$$

and

$$\sigma_d = 0.61 \times 10^{-6} C^{1/2} \sqrt{\frac{\exp\left(-\frac{z_{cat}F\Psi_d}{RT}\right) - 1}{z_{cat}} + \frac{\exp\left(\frac{z_{an}F\Psi_d}{RT}\right) - 1}{z_{an}}}, \tag{B7}$$

with

$$\sigma_s + \sigma_a + \sigma_\beta + \sigma_d = 0. \tag{B8}$$

In these equations:

Ψ_s, Ψ_a Ψ_β and Ψ_d are the electric potentials (V) at the planes 's', 'a', 'β' and 'd', respectively.

G_{sa}, $G_{a\beta}$ and $G_{\beta d}$ are the electric capacitances (mol V^{-1} m^{-2}) corresponding to the space between the planes 's' and 'a', 'a' and 'β' and 'β' and 'd', respectively, σ_s, σ_a, σ_β and σ_d are the electric charges (mol m^{-2}) localized at the planes 's', 'a', 'β' and 'd', respectively. Quantities in square brackets are concentrations of ions in solution used in place of the activities when they are small enough and a_i are the activities of specifically adsorbed ions.

N_S is the maximum surface charge density (mol m^{-2}).

N_T is the maximum adsorption density of specific adsorbed ions (mol m^{-2}) located in the plane 'a'.

K_H, K_{OH}, K_i, K_{cat} and K_{an} are the binding constants (litre mol^{-1}) of protons, hydroxyl groups, specific adsorbed ions and non-specific adsorbed cations and anions, respectively.

z_{cat} and z_{an} are the valence of the cation and anion of the background electrolyte.

Z_i is the charge of the i^{th} specifically adsorbed ion.

F is the Faraday constant (96 485 C mol^{-1}), R is the gas constant (8.314 J mol^{-1} K^{-1}) and T is the temperature (K). Equation (B7) is taken from Barrow and co-workers for asymmetric electrolytes (Barrow *et al*., 1980).

Appendix 3: Tables A1 and A2

Table A1 Data used to estimate the mean specific surface area

Mineral	Specific surface area/$m^2\ g^{-1}$	Reference
Goethite	31	Kavanagh *et al*. (1980)
	32, 28, 17, 81, 32	Hingston *et al*. (1972)
	42	Watson *et al*. (1973)
	31.2	Goldberg & Glaubig (1985)
	81	Bowden *et al*. (1980)
	120	Parfitt (1977)
	90	Parfitt (1978)
	66, 170	Schwertmann & Kämpf (1985)
	Mean value for Fe-oxides: 58.6 ~ 59	
Gibbsite	48	Muljadi *et al*. (1966)
	47	Hingston *et al*. (1972)
	58	Datta & Kunal Gosh (1992)
Al_2O_3	69.6	Goldberg & Glaubig (1988)
	117	Holl & Stumm (1976)
	96.9	Goldberg & Glaubig (1985)
	100	He *et al*. (1997)
	108	Kummert & Stumm (1980)
	Mean value for Al-oxides: 80.6 ~ 81	

Table A2 Data used to estimate the mean maximum number of specific adsorption sites, N_T

Mineral	Compound	$N_T/10^6$ mol m^{-2}	Reference
Goethite	MCPA	3.0	Kavanagh *et al*. (1980)
	2,4-D	1.0	Kavanagh *et al*. (1980)
	2,4-D	2.38	Watson *et al*. (1973)
	Phosphate	2.5	Strauss *et al*. (1997)
	Phosphate	2.43	Bowden *et al*. (1980)
	Citrate	1.74	Bowden *et al*. (1980)
	Selenite	2.71	Bowden *et al*. (1980)
Haematite	Phosphate	0.8–4.41	Bowden *et al*. (1980)
	Mean value Fe-oxides	2.33	
Gibbsite	Phosphate	3.12	Muljadi *et al*. (1966)
Al_2O_3	Silicate	3.57	Goldberg & Glaubig (1988)
	B	0.07	Goldberg & Glaubig (1985)
	B	2.2	Holl & Stumm (1976)
	B	1.96	Goldberg & Glaubig (1988)
	Mean value Al-oxides	2.18	

Appendix 4: Statistical tests

Scaled total error	Scaled root mean squared error	Model efficiency
$\mathrm{TE} = \frac{\sum_{i=1}^{n} \lVert P_i - O_i \rVert}{\sum_{i=1}^{n} O_i}$	$\mathrm{SRMSE} = \frac{1}{O_m}\sqrt{\frac{\sum_{i=1}^{n} (P_i - O_i)^2}{n}}$	$\mathrm{ME} = \frac{\sum_{i=1}^{n} (O_i - O_m)^2 - \sum_{i=1}^{n} (P_i - O_i)^2}{\sum_{i=1}^{n} (O_i - O_m)^2}$
The smaller the TE, the better is the simulation	The smaller the SRMSE, the better is the simulation	ME varies from 1 to -∞ The ideal case corresponds to ME=1

O_i and P_i are the observed and calculated values of adsorbed amounts. n is the number of observations and O_m is the mean value of observed data.

